IL NUOVO CIMENTO Vol. XXIV, N. 1 1° Aprile 1962

Photon Production in Proton-Proton Collisions at 23.1 GeV.

M. Fidecaro, G. Finocchiaro (*), G. Gatti (**),
G. Giacomelli (***), W. C. Middelkoop and T. Yamagata (**)
CERN - Geneva

(ricevuto il 22 Novembre 1961)

Summary. — The energy spectra of photons produced in p-p collisions at 23.1 GeV proton kinetic energy have been measured at the laboratory angles of 1.75°, 3°, 6°, 10°, 16° and 27° by means of a lead glass total absorption Čerenkov counter. A strong, energy-dependent, anisotropy in the c.m. system is found. The π^0 laboratory energy spectra have been calculated from the experimental γ-ray spectra. Measurements of the photons produced at the three smallest angles in p-Be and p-Al collisions at 23.1 GeV indicate a production cross-section per nucleon smaller by a factor 1.4 and 1.9, respectively, compared to the free nucleon case. The photon yield as function of the incident proton energy has been studied at 6° laboratory angle in the p-Be collision. The comparison of our experimental values with a statistical model shows that the model predicts well the total photon production cross-section and the c.m. energy spectrum averaged over the total solid angle. The angular distribution is more anysotropic than the limiting one predicted by a statistical model with angular momentum conservation.

(*) On leave from the University of Roma, Roma.
(**) Now at Frascati National Laboratories, Frascati.
(***) On leave from the University of Bologna, Bologna.
(**) Ford Foundation Fellow. Now at the University of Tokyo, Tokyo.

1. – Introduction.

The study of photons produced in a high-energy proton-proton collision is of interest as a test of production models like the statistical model (1). For the practical implications in the planning of future experiments the study of photons from proton-nuclei collisions is also of interest. The photons come mainly from the decay of the neutral pion (about 5% should come from the $\Sigma^0 \to \Lambda^0 + \gamma$ decay (1)).

We have measured the photons produced by 23.1 GeV kinetic energy protons impinging on a liquid hydrogen target at the laboratory angles of 1.75°, 3°, 6°, 10°, 16° and 27°. The photons were detected by a high-energy γ-ray telescope and their energy was measured by a total absorption lead glass Čerenkov counter (2). In this way one may measure at once the whole energy spectrum at one angle. The energy resolution of the spectrometer (about 10%) is adequate though not high. The experimental results have been transformed to the centre-of-mass system. Moreover, π^0 laboratory spectra have been calculated from the γ-ray spectra. We have also measured the photon spectra produced in p-Be and p-Al collisions.

2. – Apparatus and experimental procedure.

A 23.1 GeV proton beam was obtained by scattering of the internal proton beam of the CERN Proton Synchrotron (PS) on a beryllium target (3). Figure 1 shows the beam layout. The beam emerged at an angle of 20 mrad, with respect to the internal beam direction, was deflected by a PS magnet unit, and, after escaping from the PS vacuum chamber, passed through a pair of quadrupoles, an iron collimator 1 cm wide, 6 cm high and 150 cm long, and was finally bent over 20 mrad by a 2 m long bending magnet. A second iron collimator 1 cm wide, 8 cm high and 150 cm long, the exit of which was

(1) R. HAGEDORN: *Nuovo Cimento*, **15**, 434 (1960); F. CERULUS and R. HAGEDORN: *Suppl. Nuovo Cimento*, **9**, 646, 659 (1958); J. VON BEHR and R. HAGEDORN: CERN report 60-20 (1960); R. HAGEDORN: *Proc. of the International Conf. on Theoretical Aspects of Very High-Energy Phenomena*, in CERN-report 61-22, p. 183 (1961); T. ERICSON: CERN report 61-22, p. 205 (1961); F. CERULUS: *CERN Report* 61-22, p. 212 (1961); E. C. G. SUDARSHAN: CERN report 61-22, p. 221 (1961).

(2) G. GATTI, G. GIACOMELLI, W. A. LOVE, W. C. MIDDELKOOP and T. YAMAGATA: *Rev. Sci. Instr.*, **32**, 949 (1961).

(3) B. DAYTON, W. KOCK, M. NICOLIĆ, H. WINZELER, J. C. COMBE, W. M. GIBSON, W. O. LOCK, M. SCHNEEBERGER and G. VANDERHAEGHE: *Helv. Phys. Acta*, **33**, 344 (1960). We thank the members of Professor Cocconi's group for having supplied us with all the information concerning the beam.

placed 10 m from the centre of the bending magnet, defined the momentum dispersion of the proton beam to $\pm 2.5\%$. A counter telescope consisting of a scintillator, 0.4 cm diameter and 0.4 cm thick, in coincidence with a second scintillator, $2 \times 0.7 \times 0.4$ cm^3, was placed at about 3.5 m from the exit of the

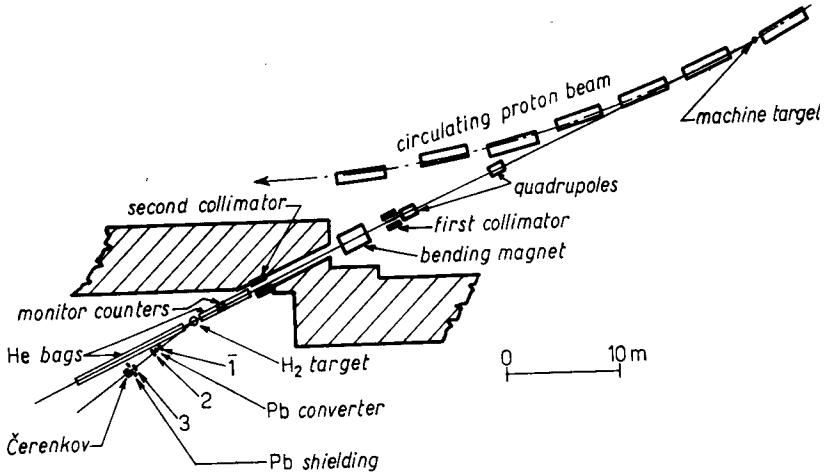

Fig. 1. – Beam layout.

last collimator. The telescope was used to optimize the currents in the magnet and the quadrupoles, to scan the shape of the beam, and to monitor the beam intensity during the experiment. The beam was 1.2 cm wide and 4.7 cm high (full width at half height). The integration of the beam shape together with the monitor provides the absolute proton intensity incident on the hydrogen target. The average intensity of the proton beam was $5 \cdot 10^5$ protons per beam pulse of $2.5 \cdot 10^{11}$ accelerated protons. The pulse duration was longer than 50 ms. At 23.1 GeV the machine repetition rate is 1 pulse every 3 s.

The hydrogen target was of the type cooled by liquid nitrogen. The appendix consistend of a vertical mylar cylinder 20 cm in diameter and 0.008 in. thick. It was surrounded by a 0.002 in. thick aluminium thermal shield. The incident proton beam as well as the produced photons, at the different angles where measurements were performed, passed through 0.009 in. thick mylar windows in the outer jacket.

The photons were detected by a high-energy γ-ray telescope consisting of an anticoincidence counter, 22 cm in diameter, a lead converter 0.5 cm thick, two coincidence counters (10×15) cm^2, and a lead glass total absorption Čerenkov counter ([2]). The Čerenkov counter was used as a photon spectrometer. The glass, 35 cm in diameter and 30 cm long, was directly viewed by seven 5 in. 58 AVP photomultipliers. The energy calibration of the counter was made by momentum-selected electrons. The counter proved to be linear up to 14 GeV, while its energy resolution is better than 10% above 5 GeV.

The position of the counters and the size of the lead converter were different at each angle. To avoid the detection of both photons from a π^0, the acceptance of the Čerenkov was restricted by a 20 cm thick lead wall with a (12.5×17.5) cm^2 window, so that the maximum accepted angle was always smaller than the minimum angle between the photons from a π^0 of the highest expected energy for each laboratory angle. This window was slightly larger than counter 3 which defines the solid angle. In order to reduce the target empty background, the proton beam passed through a helium atmosphere both before

TABLE I. – *Some parameters of the geometry used for the photon telescope.*

Laboratory angle	C.m. angle	Solid angle (10^{-4} sr)	Size of converter (cm^2)	Distance from hydrogen target to	
				counter 2 (cm)	counter 3 (cm)
1.75°	12.5°	0.82	7 ·13	550	1350
3°	21.3°	1.50	7 ·13	450	1000
6°	41.1°	2.23	8.5·13	450	820
10°	64.1°	3.55	10 ·15	400	650
16°	90.3°	7.41	10 ·15	320	450
27°	119.1°	16.60	10 ·15	250	300

and after the hydrogen target. In addition, the length of the beam path seen by the telescope, determined by the last (10×15) cm^2 counter together with the lead converter, was made as short as possible, compatible with a convenient counting rate ($(5 \div 10)$ counts per burst).

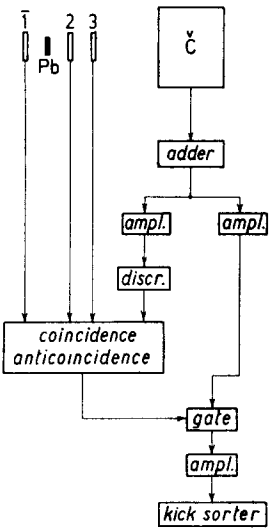

Fig. 2. – Block diagram of electronics.

Details of the geometry used at each angle are given in Table I.

This system has a photon detection efficiency of 50% essentially constant over the photon spectrum. It is highly directional and very efficient in suppressing background from other particles both neutral and charged.

A simplified diagram of the electronics is shown in Fig. 2. A coincidence between the counters 23C in the absence of an anticoincidence pulse from counter 1 opened a linear gate through which the Čerenkov pulse passed to be recorded on a 100-channel CDC kick sorter.

Runs with full target were alternated with empty target runs. We measured several times singles, ac-

cidentals and rates with the lead converter removed. The stability in the energy calibration was systematically checked both with a stabilized pulser simulating a pulse from the Čerenkov counter, and with a beam of fast μ-mesons which lose in the lead glass 250 MeV.

Data are obtained in the form of kicksorter spectra. They were corrected, for target empty background (changing from 17% at $1\frac{3}{4}°$ to 37% at 27°), for conversion of photons in counter 2 ($\sim 2\%$) and in the space between the target and the anticoincidence counter ($\sim 2\%$), for background counting rate without the lead converter ($\sim 3.5\%$), for analyser losses ($\sim 2\%$) and monitor losses ($\sim 2.5\%$); random coincidences were negligible.

A major uncertainty is the energy scale uncertainty of $\pm 3\%$ which causes an error in the differential cross-sections which changes from $\pm 4\%$ at 2 GeV to $\pm 12\%$ at 8 GeV for the 6° angle and, due to the uncertainty in the energy bias, a $(5 \div 8)\%$ error in the total cross-section measurement. Proton monitor inaccuracy introduces an error of about $\pm 3\%$. Geometrical uncertainties are negligible.

Finally there is an error resulting from the finite angle between the electron and positron of the pair. This results in an increase of the effective solid angle for photon detection and an occasional loss of an electron or positron in the lead in front of the Čerenkov counter. The two effects tend to cancel each other. The resultant effect is most important for the low-energy photons at the smallest angles, since the correction is inversely proportional to the photon energy and proportional to the distance between the lead converter and counter 3. A conservative estimate, based on the angular distribution calculated by BORSELLINO [4] shows the correction to be smaller than 5% for 1 GeV photons at $1\frac{3}{4}°$. This correction has been neglected.

At each angle the final spectrum has a total statistics of between 8000 and 20000 counts. Since the spectra are exponential, the low-energy kicksorter channels have a high number of counts (statistics of better than 5%), while the high-energy channels have few counts. To improve the statistical accuracy, we have grouped together several high-energy channels.

It is estimated that the total accuracy of the differential cross-sections derived from our data is between ± 10 and $\pm 15\%$.

3. – Results and discussion.

The results are presented in semilogarithmic graphical form. Errors quoted are standard deviations and include uncertainties due to counting statistics, as well as the uncertainties quoted in the previous section. In the same graphs

[4] A. BORSELLINO: *Phys. Rev.*, **89**, 1023 (1953).

we have also plotted the predictions of the statistical model transformed to the laboratory system with the hypothesis of isotropy in the centre-of-mass system. In addition, we have used a total p-p inelastic cross-section of 32 mb [5] to make the comparison possible, since the predictions of the statistical model are expressed per proton-proton interaction.

Figure 3 shows the photon spectra produced in proton-proton collisions at 23.1 GeV kinetic energy at the laboratory angles of 1.75°, 3°, 6°, 10°, 16°

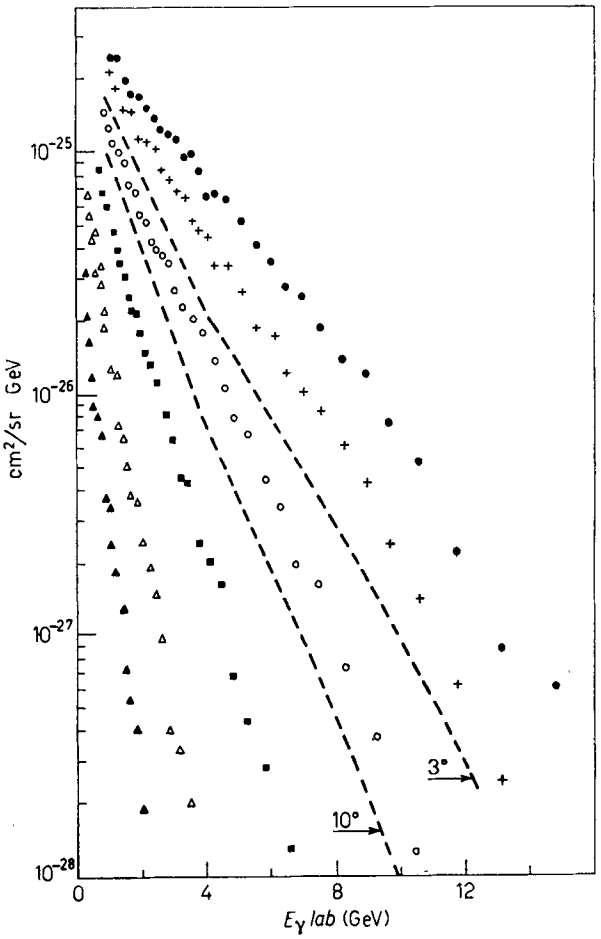

Fig. 3. – Laboratory energy spectra of photons produced in p-p collisions at 23.1 GeV proton kinetic energy. Dashed curves are 3° and 10° spectra predicted by a statistical model calculation at 25 GeV: ● 1,75° lab., + 3° lab., ○ 6° lab., ■ 10° lab., △ 16° lab., ▲ 27° lab.

---

[5] G. COCCONI and D. O. MORRISON: private communications; A. BARBARO-GALTIERI, A. MANFREDINI, B. QUASSIATI, C. CASTAGNOLI, A. GAINOTTI and T. ORTALLI: *Nuovo Cimento*, **21**, 469 (1961).

and 27°. The two dotted curves are the predictions of the statistical model for 25 GeV collisions at the laboratory angles of 3° and 10°. It is immediately seen that while the shape of the spectra is reasonably well predicted, the angular distribution is not. This last conclusion is better seen in Fig. 4, where the cross-section for the production of photons of energy higher than 0.65 GeV is plotted as a function of the photon laboratory angle both from our results and from the statistical calculations.

The experimental results have been transformed to the centre-of-mass frame by means of the following kinematical relations:

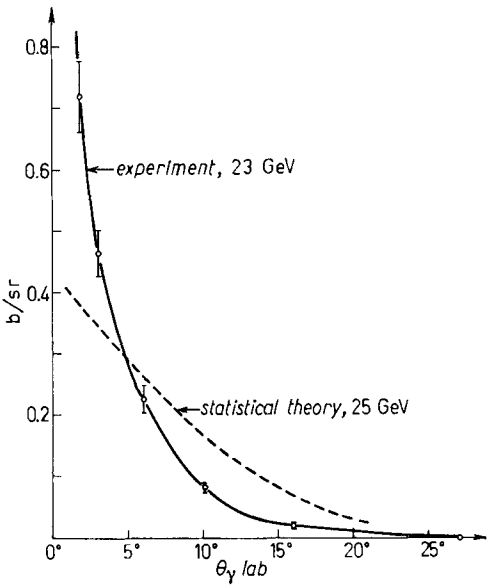

Fig. 4. – Laboratory angular distribution for the photons of energy larger than 0.65 GeV.

$$(1) \qquad \frac{\mathrm{d}^2\sigma(k^*,\theta^*)}{\mathrm{d}k^*\,\mathrm{d}\Omega^*} = \gamma(1-\beta\cos\theta)\,\frac{\mathrm{d}^2\sigma(k,\theta)}{\mathrm{d}k\,\mathrm{d}\Omega}\,, \qquad k^* = k\gamma(1-\beta\cos\theta)\,,$$

where θ and k are the angle of emission and the energy of the photons in the laboratory system, respectively; θ^* and k^* are the corresponding quantities in the c.m. frame. $\beta = v/c$ and $\gamma = (1-\beta^2)^{-\frac{1}{2}}$ define the motion of the c.m. system with respect to the laboratory system ($\gamma = 3.64$ in our case). Figures 5 and 6 show the results of the transformation. In the c.m. there is a large energy-dependent anisotropy. Table II gives the differential cross-sections averaged over c.m. angles for different c.m. energies as derived from our experimental values. These values are plotted in Fig. 7, together with the curve predicted by the statistical model; the agreement is good. It should be emphasized that the statistical model calculations as performed by HAGEDORN *et al.* [1] only pretend to give the particle production as a function of energy in the c.m. system. The additional assumption of isotropy in the c.m. was introduced as the simplest hypothesis needed to transform the c.m. spectar to the laboratory system. The effects of angular momentum conservation were not included in the theory of Hagedorn *et al.* Its introduction will yield a c.m. angular distribution forward-backward peaked, but not more than a limiting distribution $1/\sin\theta^*$ [6]. It is evident from Fig. 6 that this is not

[6] T. ERICSON: *Nuovo Cimento*, **21**, 605 (1961).

the case for photons of c.m. energies of 0.4 GeV or higher, which thus cannot be explained by a purely statistical model.

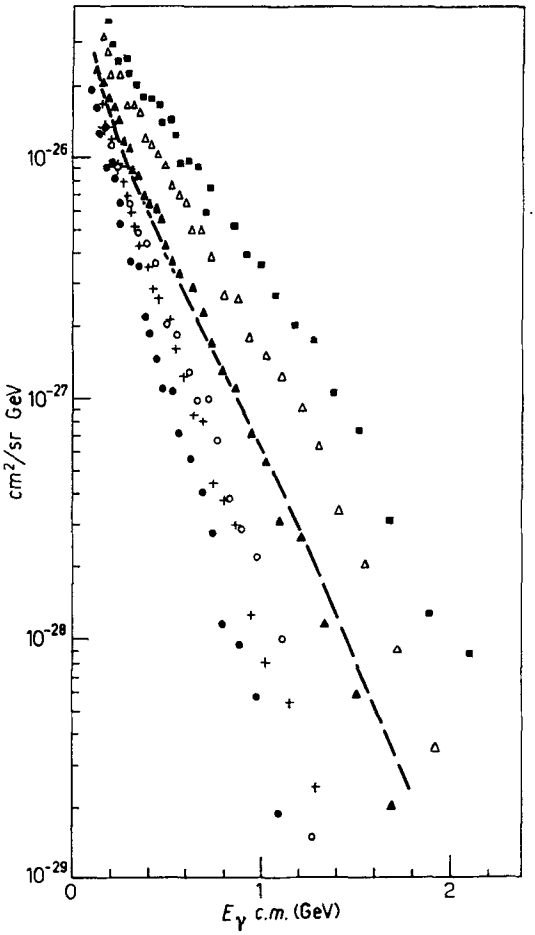

Fig. 5. – Photon spectra transformed to the c.m. system. Dotted line is the prediction of the statistical model at 25 GeV proton kinetic energy: ■ 21.5° c.m., △ 21.3° c.m., ▲ 41.1° c.m., + 64.1° c.m., ● 90.3° c.m., ○ 0119.1° c.m.

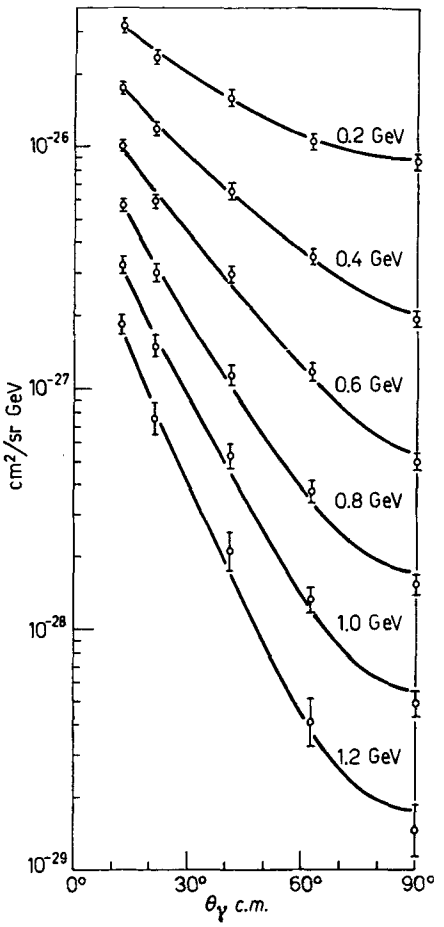

Fig. 6. – C.m. angular distributions for photons of different c.m. energies. (Full lines are drawn only to connect the points together.)

Since the γ-rays produced in p-p collisions come mainly from the decay of the π^0-meson, it is possible to derive the π^0 spectra from the photon spectra. The derivation is facilitated by the high photon energies, because the direction of a high-energy photon is essentially that of the π^0. For the transformation

we have used the following formula (7):

$$(2) \qquad \frac{\mathrm{d}^2\sigma_\pi(p,\theta_\pi)}{\mathrm{d}p\,\mathrm{d}\Omega_\pi} = -\frac{p}{2}\left[\frac{\partial}{\partial k}\left(\frac{\mathrm{d}^2\sigma_\gamma(k,\theta_\gamma)}{\mathrm{d}k\,\mathrm{d}\Omega_\gamma}\right)\right]_{\substack{k=p \\ \theta_\gamma=\theta_\pi}},$$

where all quantities are expressed in the laboratory system and p is the momentum of the neutral pion. It contains the approximation that the average of $\mathrm{d}^2\sigma_\pi/\mathrm{d}p\,\mathrm{d}\Omega_\pi$ over a cone of semi-aperture $\Delta\theta$ around the π^0 direction is replaced by the value of $\mathrm{d}^2\sigma_\pi/\mathrm{d}p\,\mathrm{d}\Omega_\pi$

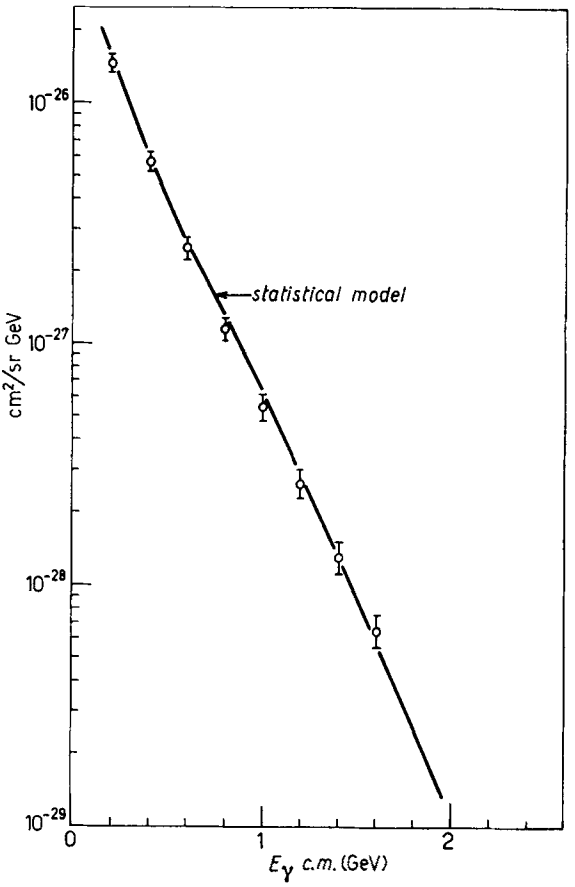

Fig. 7. – Photon c.m. energy spectrum integrated over angles. Solid line is the prediction of the statistical model calculation at 25 GeV.

TABLE II. – *Center of mass cross-sections for photon production averaged over all center of mass angles. Errors are standard deviations and include statistical as well as estimated errors for the integration over energies.*

C.m. energy (GeV)	Cross-section (mb/GeV sr)
0.2	14.7 ± 1.5
0.4	5.7 ± 0.6
0.6	2.54 ± 0.30
0.8	1.16 ± 0.15
1.0	0.55 ± 0.08
1.2	0.262 ± 0.045
1.4	0.131 ± 0.023
1.6	0.065 ± 0.013

(7) R. M. STERNHEIMER: *Phys. Rev.*, **99**, 277 (1955).

at θ_π. The value of $\Delta\theta$ is given as $m_\pi/2k$ and amounts only to 1°56′ at $k = 2$ GeV/c. Hence this approximation seems to be reasonable for high-energy pions.

Figure 8 shows the π^0 spectra in the laboratory system as derived from our experimental results. The spectra are not reliable below 2 GeV/c; we have estimated that the error is smaller than $\pm 30\%$ above 2 GeV (see Appendix). Our spectra agree reasonably well with the spectra of the charged pions measured both at CERN and at Brookhaven [8]. The comparison can only be qualitative also because charged pions were produced in internal beryllium or aluminium targets and the number of interacting protons was poorly known.

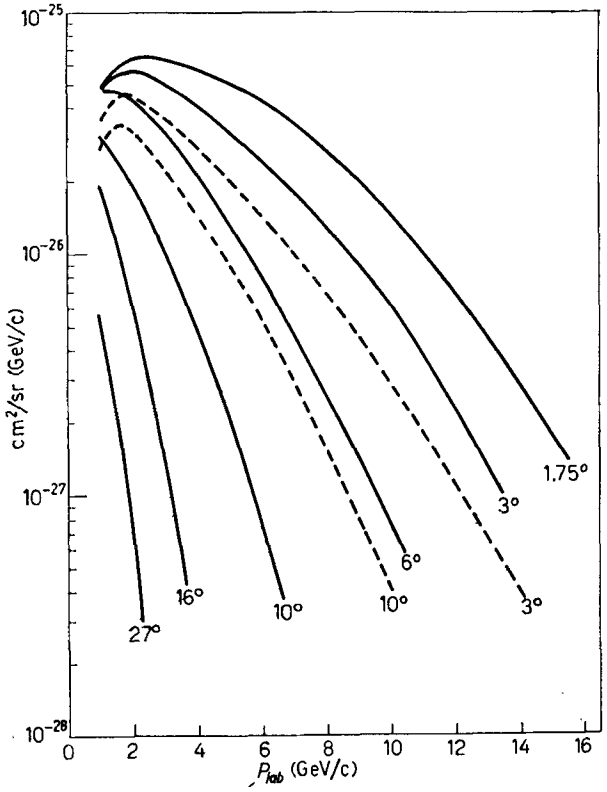

Fig. 8. – Laboratory π^0 spectra derived from the measured photon spectra. Dashed curves are 3° and 10° spectra predicted by a statistical model calculation at 25 GeV.

4. – Photon production in proton-nuclei collisions.

The geometry used for the measurement of photons produced in p-Be and p-Al collisions was the same as that used in the p-p case. Both beryllium and aluminium targets were 3.65 g cm^{-2} thick. Figure 9 shows the experimental spectra of γ-rays produced in p-Be collisions at 23.1 GeV kinetic energy at

([8]) G. COCCONI: *Proc. of the 1960 Ann. Int. Conf. on High-Energy Physics* (Rochester) (New York, 1960); W. F. BAKER, R. L. COOL, E. W. JENKINS, T. F. KYCIA, S. J. LINDENBAUM, W. A. LOVE, D. LÜERS, J. A. NIEDERER, S. OZAKI, A. L. READ, J. J. RUSSELL and L. C. L. YUAN: *Phys. Rev. Lett.*, **7**, 101 (1961).

the laboratory angles of 1.75°, 3° and 6°. The comparison of Fig. 9 with Fig. 3 shows that the spectra from p-p and p-Be collisions are quite similar,

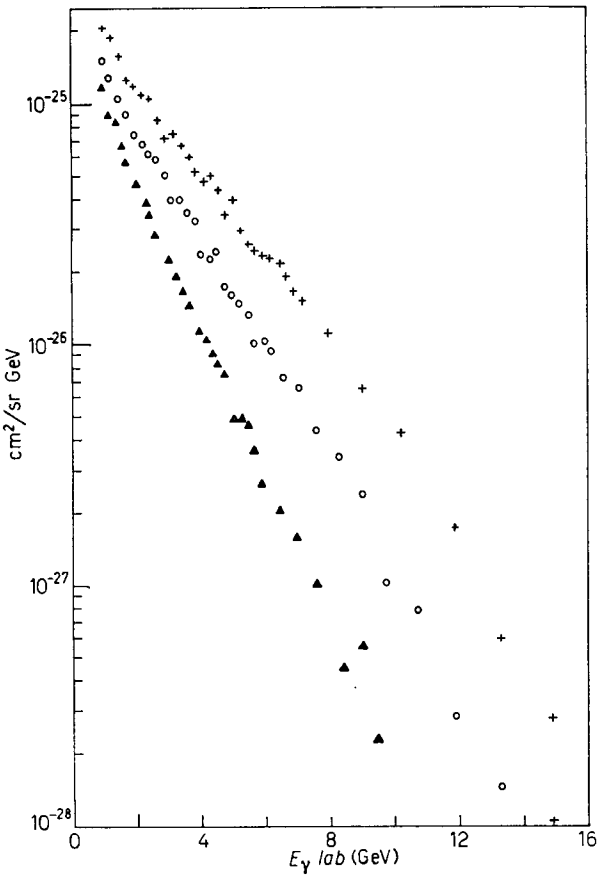

Fig. 9. – Laboratory spectra of photons produced in p-Be collision at 23.1 GeV kinetic energy. Cross-section is per nucleon: + 1.75° lab., ○ 3° lab,. ▲ 6° lab.

the only difference being in the absolute value of the cross-section: the cross-section per nucleon in the free proton case is, over the whole spectrum, about 1.4 times that of the p-Be case. There is an indication that the angular distribution in the p-Be collision is slightly broader than in the p-p collision. A

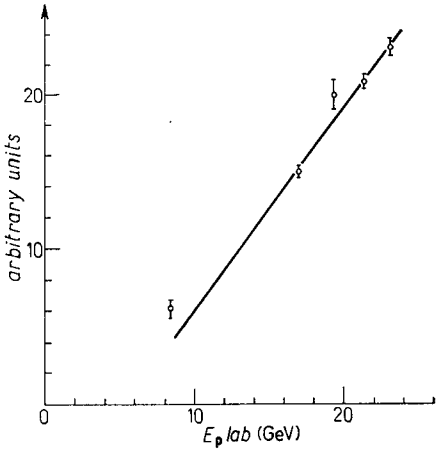

Fig. 10. – Photon yield at 6° laboratory angle in p-Be collisions as function of the incident proton kinetic energy.

similar conclusion was reached from the p-Al data; the cross-section per nucleon in p-Be is about 1.37 times that in p-Al.

Figure 10 shows the yield of photons of energy greater than 0.65 GeV for p-Be collisions, at the laboratory angle of 6°, as a function of the incident proton kinetic energy.

5. – Conclusion.

The main features of the experimental results are:

a) the energy spectra are approximately exponential;

b) the angular distribution is very much peaked forward in the laboratory system. In the c.m. system there is a strong anisotropy which increases with c.m. photon energy; and

c) spectra from p-Be and p-Al collisions are quite similar to those obtained in the p-p case, but the cross-section per nucleon is smaller by a factor of 1.4 and 1.9 respectively.

A comparison of our results with the predictions of the statistical model, as it has been developed by HAGEDORN, CERULUS and VON BEHR [1] shows that it predicts well the total cross-section and the c.m. spectrum integrated over all c.m. angles. The angular distribution is instead more pronounced than the limiting distribution predicted by the statistical model of ERICSON [6] where angular momentum effects are included.

* * *

It is a pleasure to acknowledge Professors G. BERNARDINI, R. HAGEDORN and T. ERICSON for very useful discussions. We thank Mr. G. SICHER for designing and building the hydrogen target, Mr. B. SMITH for developing the linear gate, and the PS machine group for their assistance in the setting up of the experiment and for the smooth operation of the PS machine.

APPENDIX

If in the laboratory system $dN = g(E, \theta)\, d\Omega\, dE$ is the number of π^0's emitted with total energy between E and $E + dE$ in the solid angle $d\Omega$ at an angle θ with respect to incident beam direction, the corresponding distri-

bution for the photons produced in the π^0 decay, $f(k, \theta)$, can be written

$$(A.1)\quad f(k,\theta) = \int_{k+(m^2/4k)}^{\infty} dE \int_{-1}^{1} d\cos\theta'' \int_{0}^{2\pi} d\varphi'' g(E, \theta'(\theta'', \varphi'')) \frac{\delta[(E/m)k(1-\beta\cos\theta'') - m/2]}{2\pi(E/m)(1-\beta\cos\theta'')} =$$

$$= \frac{1}{\pi} \int_{k+(m^2/4k)}^{\infty} \frac{dE}{p} \int_{0}^{2\pi} d\varphi'' g(E, \theta'(\theta''_E, \varphi'')) ,$$

where k is the energy of the photon, m, E, p, β are the mass, the total energy, the momentum, and the velocity of the π^0, respectively, while the angles are represented in Fig. 11 on a sphere of unit radius. θ''_E is given by

$$\cos\theta''_E = 1/\beta(1 - m^2/2Ek) .$$

Differentiating eq. (A.1) with respect to k, which appears in the lower limit for the integration over dE and in the argument of g via the angle θ''_E, one obtains

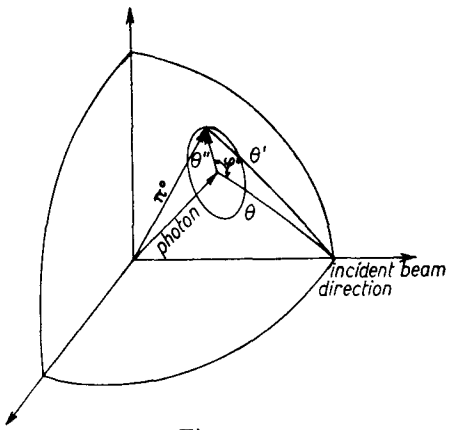

Fig. 11.

$$(A\,2)\quad \frac{\partial f(k,\theta)}{\partial k} = -\frac{2}{k} g\left(k + \frac{m^2}{4k}, \theta\right) + \frac{m^2}{2\pi k^2} \int_{k+(m^2/4k)}^{\infty} \frac{dE}{p^2} \int_{0}^{2\pi} d\varphi'' \left[\frac{\partial g[E, \theta'(\theta'', \varphi'')]}{\partial \cos\theta''}\right]_{\theta'' = \theta''_E} .$$

The integral over $d\varphi''$, considered as an integral along the circle represented in the figure, can be transformed into a surface integral; this has been evaluated by calculating at the centre of the circle the differential expression to be integrated. So eq. (A.2) becomes

$$(A.3)\quad g\left(k + \frac{m^2}{4k}, \theta\right) \simeq -\frac{k}{2}\frac{\partial f(k,\theta)}{\partial k} + \frac{m^2}{4k} \int_{k+(m^2/4k)}^{\infty} \frac{dE}{p^2} \left[2\cos\theta \frac{\partial g(E,\theta)}{\partial \cos\theta} - \sin^2\theta \frac{\partial^2 g(E,\theta)}{\partial \cos\theta^2}\right] .$$

Neglecting the last term in eq. (A.3) and $m^2/4k$ with respect to k, we obtain

$$(A.4)\qquad g(k,\theta) = -\frac{k}{2}\frac{\partial f(k,\theta)}{\partial k} .$$

This approximation (7) is equivalent, as can be seen from eq. (A.1), to neglecting the emission angle of the photons with respect to the π^0.

We have used eq. (A.4) to compute the π^0 spectra. The second term in the right-hand side of eq. (A.3) was evaluated with the $g(k, \theta)$ so obtained and taken as an estimate of the error. This error, exclusively due to the approximation in the derivation of the pion spectra from the photon spectra, was found to change from about 18% at 2 GeV to 1% at 10 GeV for $\theta = 3°$.

RIASSUNTO

Usando un contatore di Čerenkov ad assorbimento totale, abbiamo misurato gli spettri energetici dei fotoni prodotti nell'urto p-p a 23.1 GeV agli angoli di 1.75°, 3°, 6°, 10°, 16° e 27°. Nel sistema del centro di massa troviamo una forte anisotropia. Il confronto dei nostri risultati con il modello statistico mostra che questo modello predice bene la sezione d'urto totale per produzione di fotoni e lo spettro energetico mediato sugli angoli nel centro di massa; l'anisotropia è invece molto maggiore di quella massima prevedibile dal modello statistico. Dagli spettri sperimentali per fotoni sono stati calcolati gli spettri per π^0. La misura dei fotoni prodotti ai tre angoli più piccoli nelle collisioni p-Be e p-Al a 23.1 GeV mostra una sezione d'urto di produzione per nucleone più piccola rispettivamente di un fattore 1.4 e 1.9 in confronto a protoni liberi. È stata anche misurata la produzione di fotoni a 6° nell'urto p-Be per differenti energie dei protoni incidenti.